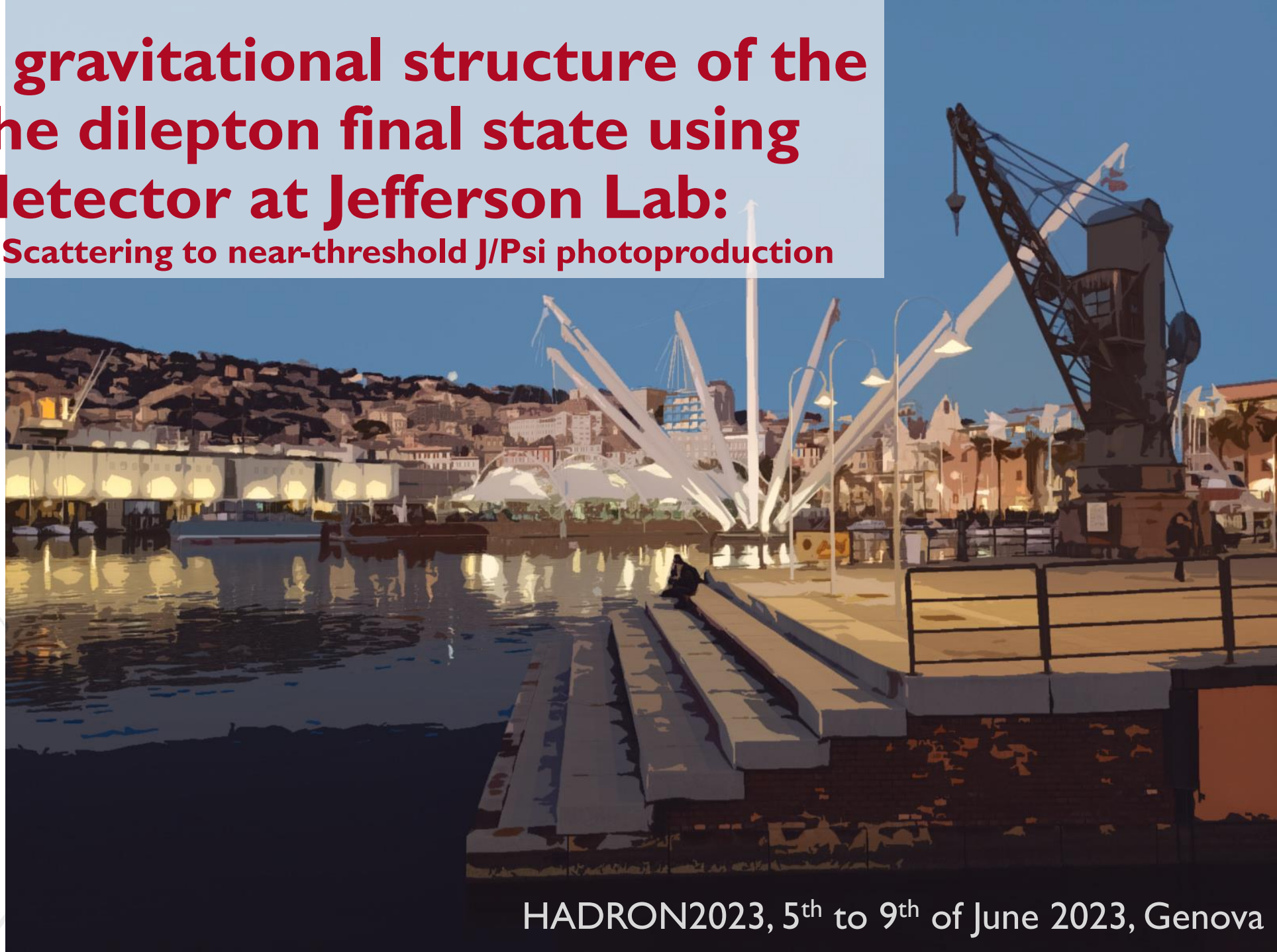


# Exploring the gravitational structure of the proton with the dilepton final state using the CLAS12 detector at Jefferson Lab:

from Timelike Compton Scattering to near-threshold J/Psi photoproduction

Pierre Chatagnon,  
for the CLAS collaboration



HADRON2023, 5<sup>th</sup> to 9<sup>th</sup> of June 2023, Genova

# Outline of the talk

I

Gravitational Form Factors and their link to Generalized Parton Distributions

II

The CLAS12 experiment at Jefferson Lab

III

Early results: First Timelike Compton Scattering measurement with CLAS12

IV

Ongoing effort : near threshold  $J/\psi$  photoproduction cross-section measurement

# Gravitational Form Factors, Generalized Parton Distributions...

## The Gravitational Form Factors, ...

- Concept introduced in the 1960s Y. Kobzarev and L. B. Okun, Gravitational Interaction Of Fermions, Zh. Eksp. Teor. Fiz. 43, 1904 (1962)  
Heinz Pagels, Energy-Momentum Structure Form Factors of Particles, Phys. Rev. 144, 1250 (1966)
- Parametrization of the matrix elements of the QCD Energy-Momentum Tensor

$$\langle p' | T_{\mu\nu}^a(0) | p \rangle = \bar{u}' \left[ A^a(t) \frac{\gamma_{\{\mu} P_{\nu\}}}{2} + B^a(t) \frac{i P_{\{\mu} \sigma_{\nu\}} \rho}{4m} + D^a(t) \frac{\Delta_\mu \Delta_\nu - g_{\mu\nu} \Delta^2}{4m} + m \bar{c}^a(t) g_{\mu\nu} \right] u$$

- Related to the spin, the mass and the force distribution in the nucleons

## ...the Generalized Partons Distributions, ...

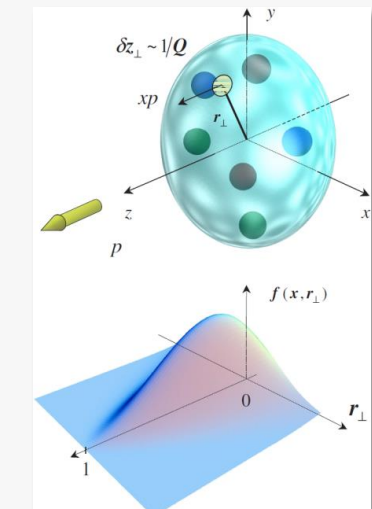
- Concept introduced in the 1990s Nonforward parton distributions A. V. Radyushkin, Phys. Rev. D 56, 5524 (1997)  
Deeply virtual Compton scattering Xiangdong Ji, Phys. Rev. D 55, 7114 (1997)
- Encoding both transverse position and longitudinal momentum of the partons in the nucleons.

$$H^q(x, b_\perp) = \int \frac{d^2 \Delta_\perp}{(2\pi)^2} e^{-ib_\perp \Delta_\perp} H^q(x, 0, -\Delta_\perp^2)$$

- Closely related to electro-magnetic FFs and PDFs

$$\int_{-1}^1 dx H^q(x, \xi, t) = F_1^q(t) \quad \int_{-1}^1 dx E^q(x, \xi, t) = F_2^q(t) \quad H^q(x, 0, 0) = \begin{cases} q(x), & x > 0 \\ -\bar{q}(-x), & x < 0 \end{cases}$$

Figure in A.V. Belitsky, A.V. Radyushkin, Unraveling hadron structure with generalized parton distributions, Physics Reports, Volume 418, Issues 1–6 2005



# ... and their link

- First x-moment of the GPDs

$$\int_{-1}^1 dx \ x H^q(x, \xi, t) = A^q(t) + \xi^2 D^q(t) \quad \int_{-1}^1 dx \ x E^q(x, \xi, t) = B^q(t) - \xi^2 D^q(t)$$

- Link with the spin composition of the nucleon (aka the “spin puzzle”) using the Ji’s sum rule:

$$\frac{1}{2} = J_Q + J_G \longrightarrow J_Q = \sum_q \frac{1}{2} \int_{-1}^1 dx \ x (H^q(x, \xi, 0) + E^q(x, \xi, 0)) = \sum_q \frac{1}{2} (A^q(0) + B^q(0))$$

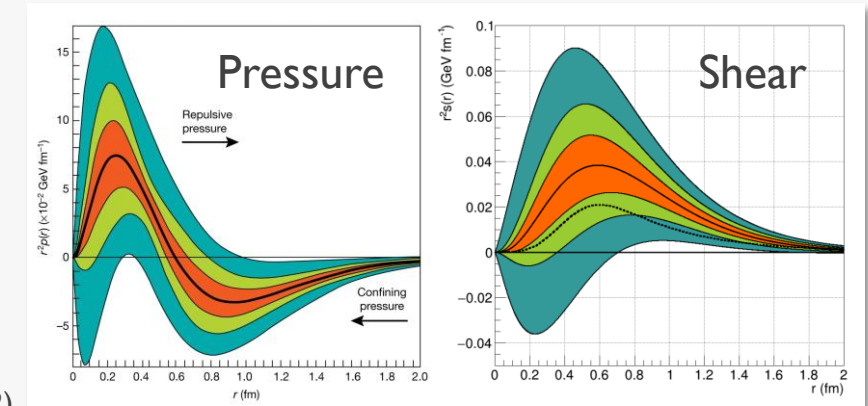
## A path toward the experimental extraction of GFFs

- Relations between GPDs and GFFs established in the 2000s

Ji, Xiang-Dong , Gauge-Invariant Decomposition of Nucleon Spin, Phys. Rev. Lett. 78, 610–613 (1997)  
 Polyakov, M. V. Generalized parton distributions and strong forces inside nucleons and nuclei. Phys. Lett. B 555, 57–62 (2003)

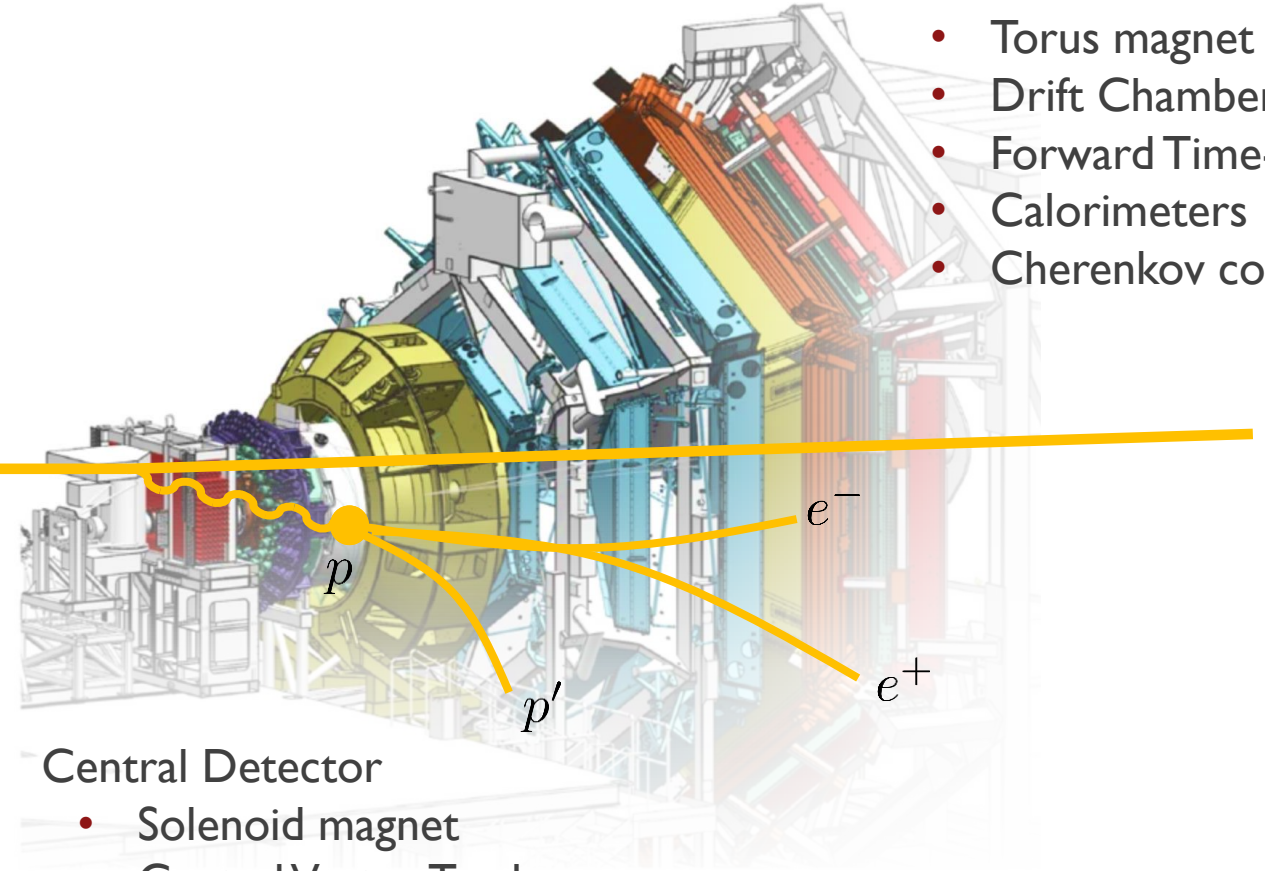
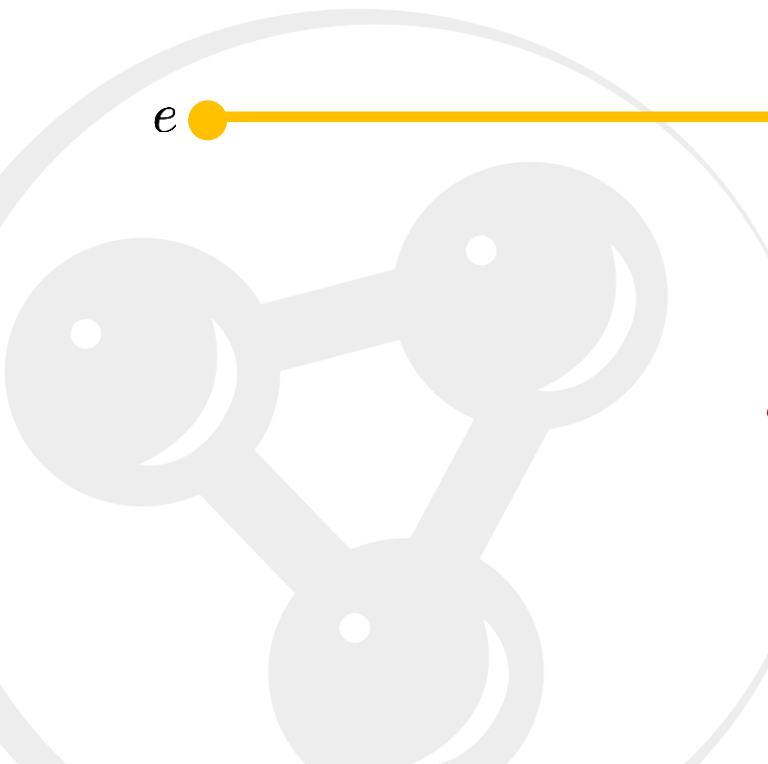
- Since then, the fields has been growing rapidly both theoretically and experimentally

Burkert, V.D. Burkert, L. Elouadrhiri, F.Girod, The pressure distribution inside the proton. Nature 557, 396–399 (2018)  
 K. A. Mamo and I. Zahed, J/ψ near threshold in holographic QCD: A and D gravitational form factors, Phys. Rev. D 106, 086004 (2022)  
 Duran, B., Meziani, ZE., Joosten, S. et al. Determining the gluonic gravitational form factors of the proton. Nature 615, 813–816 (2023)



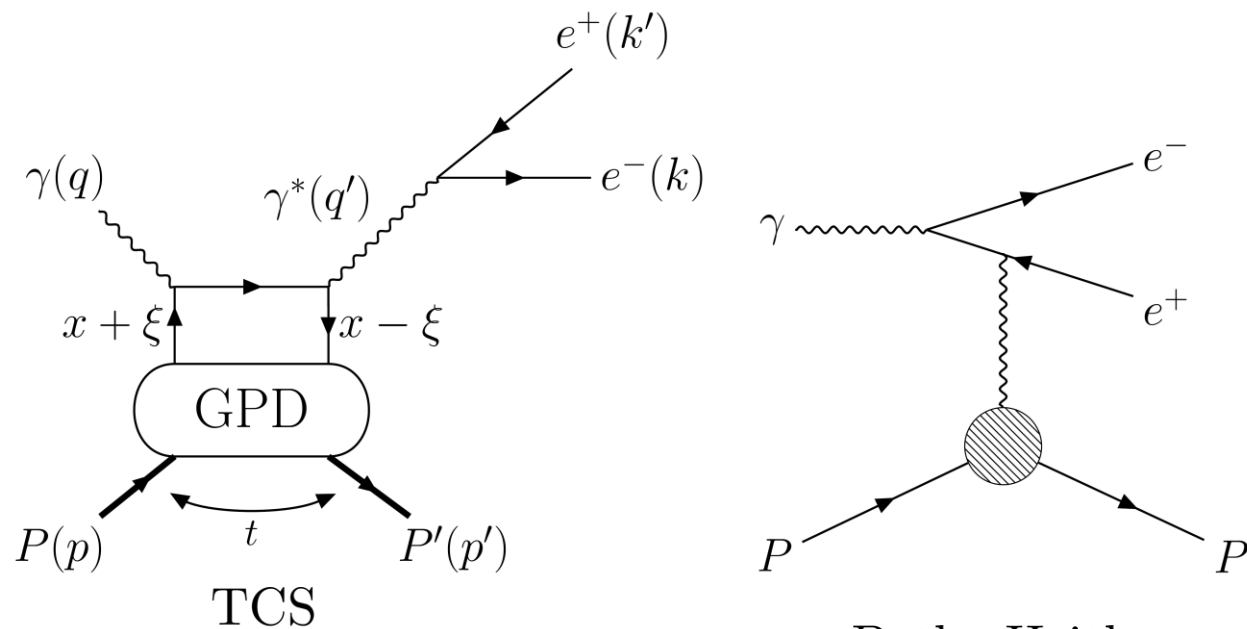
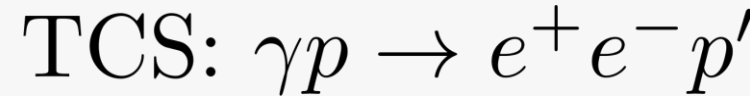
Figures in Burkert et al., The pressure distribution inside the proton. Nature 557, 396–399 (2018) and Burkert et al. arXiv:2104.02031 (2021)

# Measuring the dilepton final state with the CLAS12 experiment at Jefferson Lab

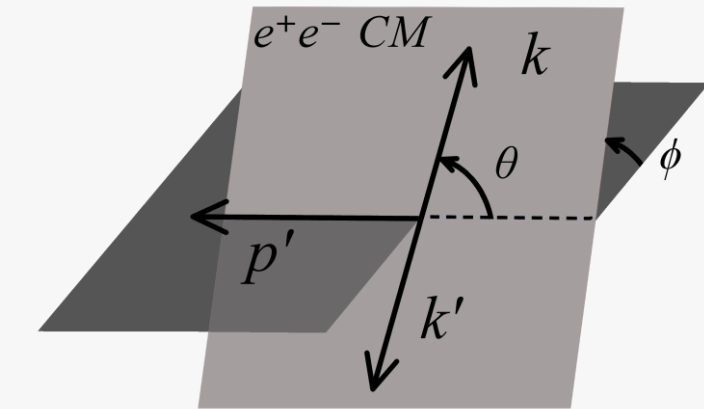


- Forward Detector (6 sectors)
  - Torus magnet
  - Drift Chambers
  - Forward Time-of-Flight
  - Calorimeters
  - Cherenkov counters
- Central Detector
  - Solenoid magnet
  - Central Vertex Tracker
  - Central Time-of-Flight
  - Central Neutron detector

# Timelike Compton Scattering reaction and kinematics



(factorization regime,  $-t/Q'^2 \ll 1$ )



$$\begin{aligned} -t &= (p - p')^2 \\ Q'^2 &= (k + k')^2 \end{aligned}$$

$$\begin{aligned} L &= [(q - k)^2 - m_l^2][(q - k')^2 - m_l^2] \\ L_0 &= (Q'^2 \sin^2 \theta)/4 \end{aligned}$$

# TCS interference cross-section formulae, CFFs and GFFs

## TCS unpolarized cross-section

Formulae and notations of Berger, Diehl, Pire, Eur.Phys.J.C23:675-689,2002

$$\frac{d^4\sigma_{INT}}{dQ'^2 dt d\Omega} \propto \frac{L_0}{L} \left[ \cos(\phi) \frac{1 + \cos^2(\theta)}{\sin(\theta)} \text{Re}\mathcal{H} + \dots \right]$$

## Compton Form Factors (CFFs)

$$\mathcal{H} = \int_{-1}^1 dx H(x, \xi, t) \left( \frac{1}{\xi - x - i\epsilon} - \frac{1}{\xi + x - i\epsilon} \right)$$

## Dispersion relation and link to GFFs

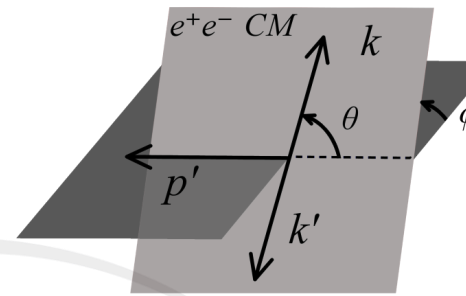
- Angular dependence of the TCS cross-section gives access to the real part of  $\mathcal{H}$ .
- This quantity is not well constrained by existing DVCS data (accessed in cross-section mostly).
- $\text{Re}(\mathcal{H})$  is related to the GFFs  $D$ , itself related to the mechanical properties of the nucleon:

$$\text{Re}\mathcal{H}(\xi, t) = \mathcal{P} \int_{-1}^1 dx \left( \frac{1}{\xi - x} - \frac{1}{\xi + x} \right) \text{Im}\mathcal{H}(\xi, t) + \Delta(t) \longrightarrow \Delta(t) \propto D^Q(t) \propto \int d^3\mathbf{r} p(r) \frac{j_0(r\sqrt{-t})}{t}$$

# The TCS Forward/Backward asymmetry

Forward/Backward correspondence:

$$k \leftrightarrow k' \iff (\theta, \phi) \leftrightarrow (180^\circ - \theta, 180^\circ + \phi)$$



## Effect on cross-sections

$$\frac{d\sigma_{BH}}{dQ^2 dt d\Omega} \propto \frac{1 + \cos^2 \theta}{\sin^2 \theta} \xrightarrow{FB} \frac{d\sigma_{BH}}{dQ^2 dt d\Omega}$$

$$\frac{d^4\sigma_{INT}}{dQ'^2 dt d\Omega} \propto \frac{L_0}{L} \cos(\phi) \frac{1 + \cos^2(\theta)}{\sin(\theta)} \xrightarrow{FB} -\frac{d\sigma_{INT}}{dQ^2 dt d\Omega}$$

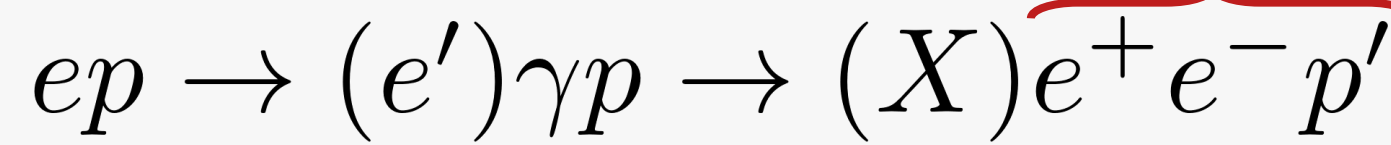
## Observable definition

$$A_{FB}(\theta_0, \phi_0) = \frac{d\sigma(\theta_0, \phi_0) - d\sigma(180^\circ - \theta_0, 180^\circ + \phi_0)}{d\sigma(\theta_0, \phi_0) + d\sigma(180^\circ - \theta_0, 180^\circ + \phi_0)} = \frac{-\frac{\alpha_{em}^3}{4\pi s^2} \frac{1}{-t} \frac{m_p}{Q'} \frac{1}{\tau\sqrt{1-\tau}} \frac{L_0}{L} \cos \phi_0 \frac{(1+\cos^2 \theta_0)}{\sin(\theta_0)} \text{Re}\mathcal{H}}{d\sigma_{BH}(\theta_0, \phi_0) + d\sigma_{BH}(180^\circ - \theta_0, 180^\circ + \phi_0)}$$

- Concept initially explored for  $J/\psi$  production (Gryniuk, Vanderhaeghen, Phys. Rev. D, 2016)
- Exploratory studies for TCS performed alongside this work
- Predictions for TCS have been published very recently + **LO radiative correction negligible**  
(Heller, Keil, Vanderhaeghen, Phys. Rev. D, 2021)

# (Quasi-)Photoproduction events selection

1) CLAS12 PID + Positron NN PID

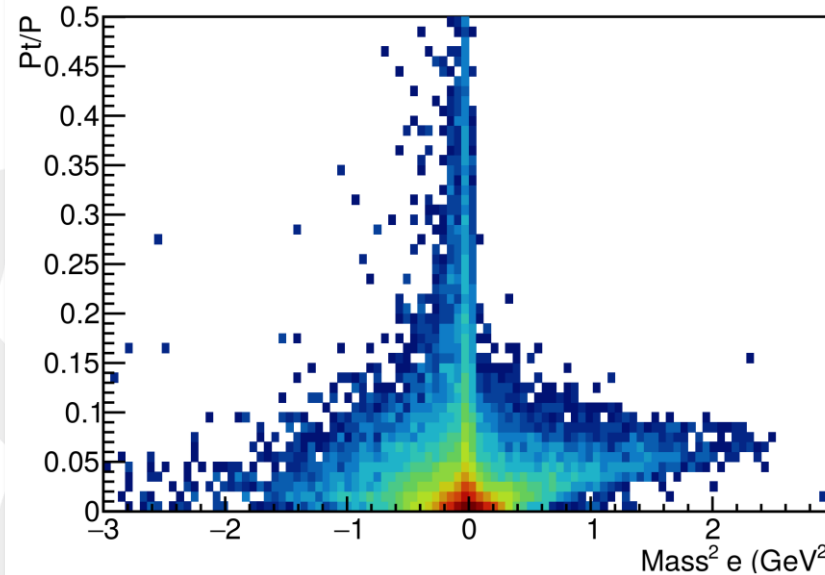


$$p_X = p_{beam} + p_p - p_{e^+} - p_{e^+} - p_{p'} \longrightarrow$$

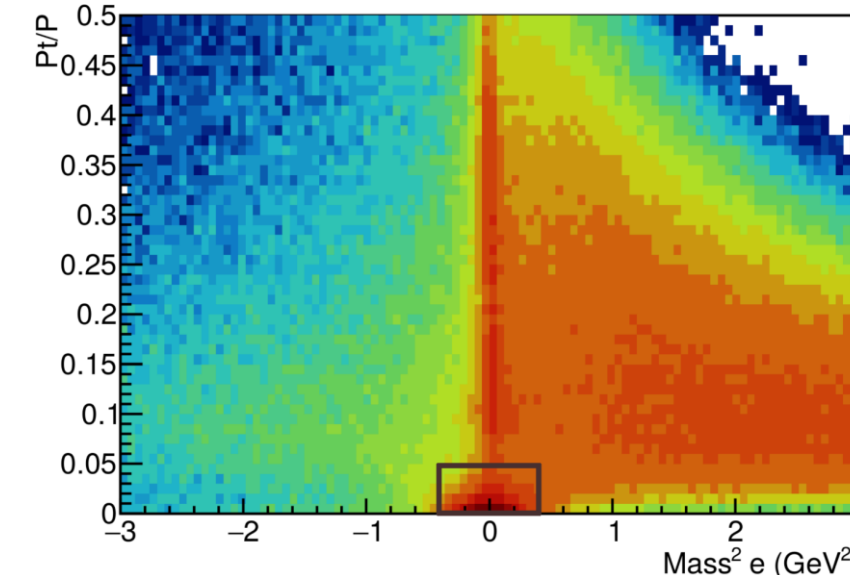
2)  $|M_X^2| < 0.4 \text{ GeV}^2$

3)  $\frac{P_{tX}}{P_X} < 0.05$   
 $\rightarrow Q^2 < 0.1 \text{ GeV}^2$

Simulation



Data



# CLAS12 dilepton invariant mass spectrum

- Data taken in Fall 2018
- 10.6 GeV beam on Liquid H<sub>2</sub> target
- Accumulated charge: 37mC or 48 fb<sup>-1</sup>

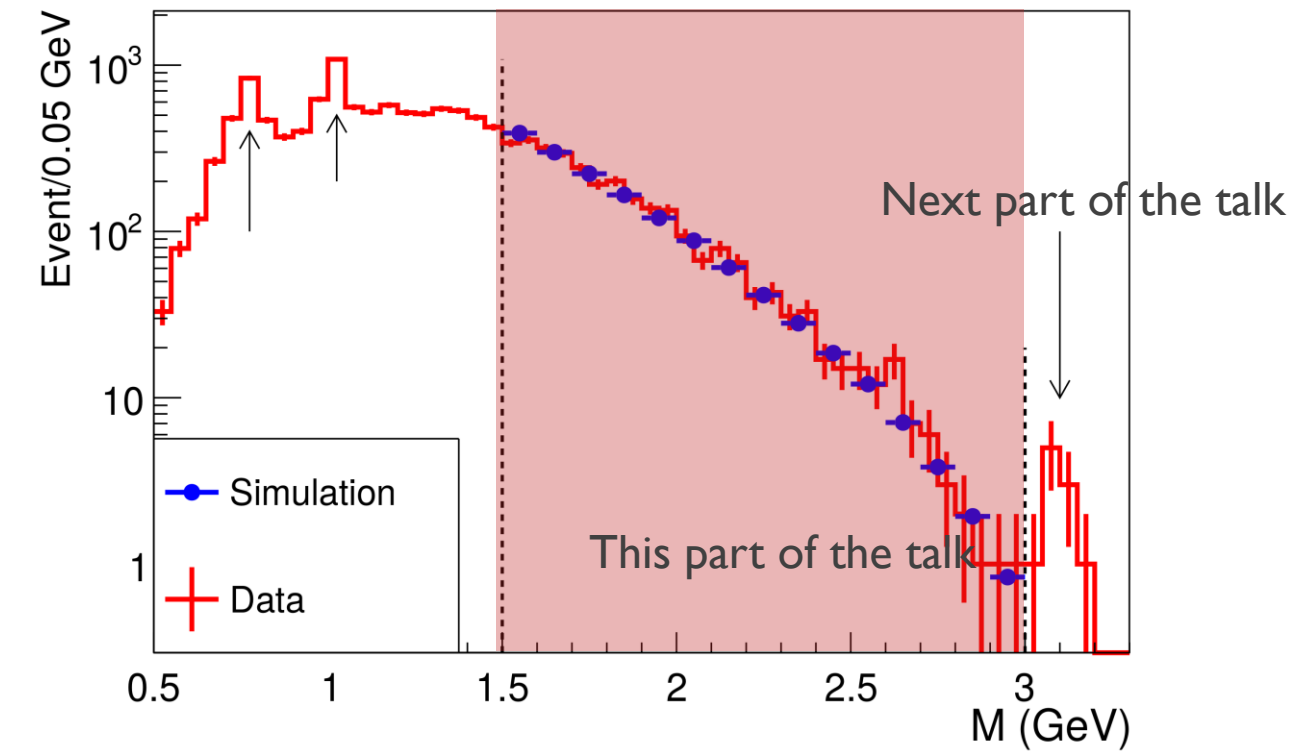
- Vector mesons peaks are visible in data:  $\omega$  (770),  $\rho$  (782),  $\phi$  (1020) and  $J/\psi$  (3096).
- Data/simulation are matching at the 15% level, up to an overall normalization factor.
- No clear contribution of higher mass vector meson production ( $\rho$  (1450),  $\rho$  (1700)).

## Phase-space for the TCS analysis

$$0.15 \text{ GeV}^2 < -t < 0.8 \text{ GeV}^2$$

$$1.5 \text{ GeV} < M_{e^+ e^-} < 3 \text{ GeV}$$

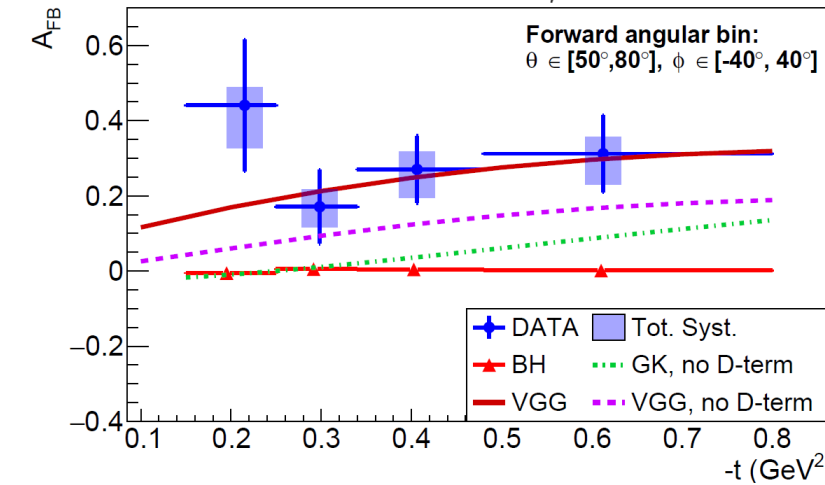
$$4 \text{ GeV} < E_\gamma < 10.6 \text{ GeV}$$



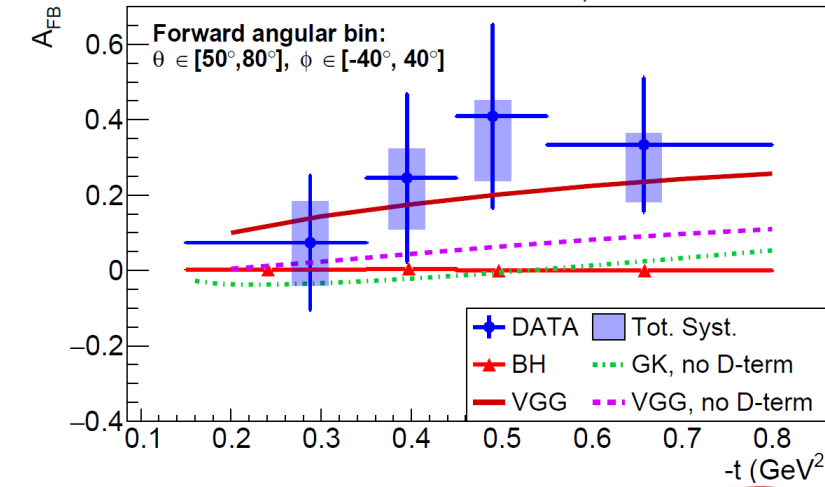
# Forward/Backward asymmetry results

- Integration over the forward angular bin :  
 $\theta \in [50^\circ, 80^\circ]$  and  $\phi \in [-40^\circ, 40^\circ]$
- Asymmetry measured in two mass bins:  
 $M \in [1.5 \text{ GeV}, 3.0 \text{ GeV}]$  and  $M \in [2.0 \text{ GeV}, 3.0 \text{ GeV}]$
- The measured asymmetry is non-zero: **evidence of signal** beyond pure BH contribution
- Measured asymmetry is better reproduced by the VGG model including the D-term
  - I. Confirmation of the importance of the D-term in the parametrization of the GPD
  2. One can use TCS data to constrain it

$\langle M \rangle = 1.8 \text{ GeV}; \langle E_\gamma \rangle = 7.24 \text{ GeV}$



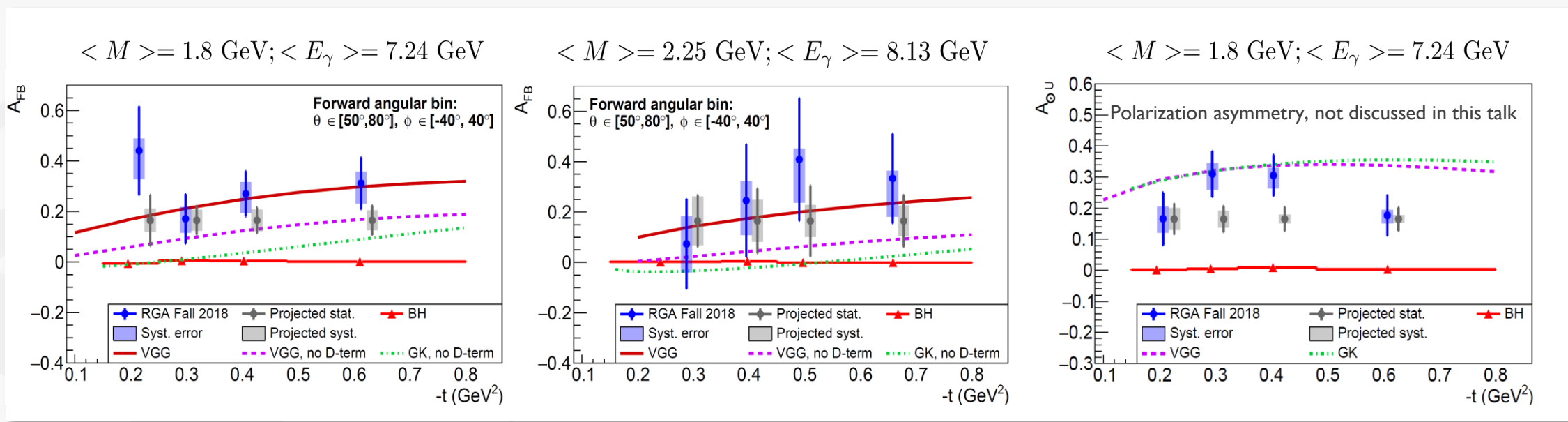
$\langle M \rangle = 2.25 \text{ GeV}; \langle E_\gamma \rangle = 8.13 \text{ GeV}$



# Perspective for TCS measurements with CLAS12

## Projections for the full proton target dataset (RG-A)

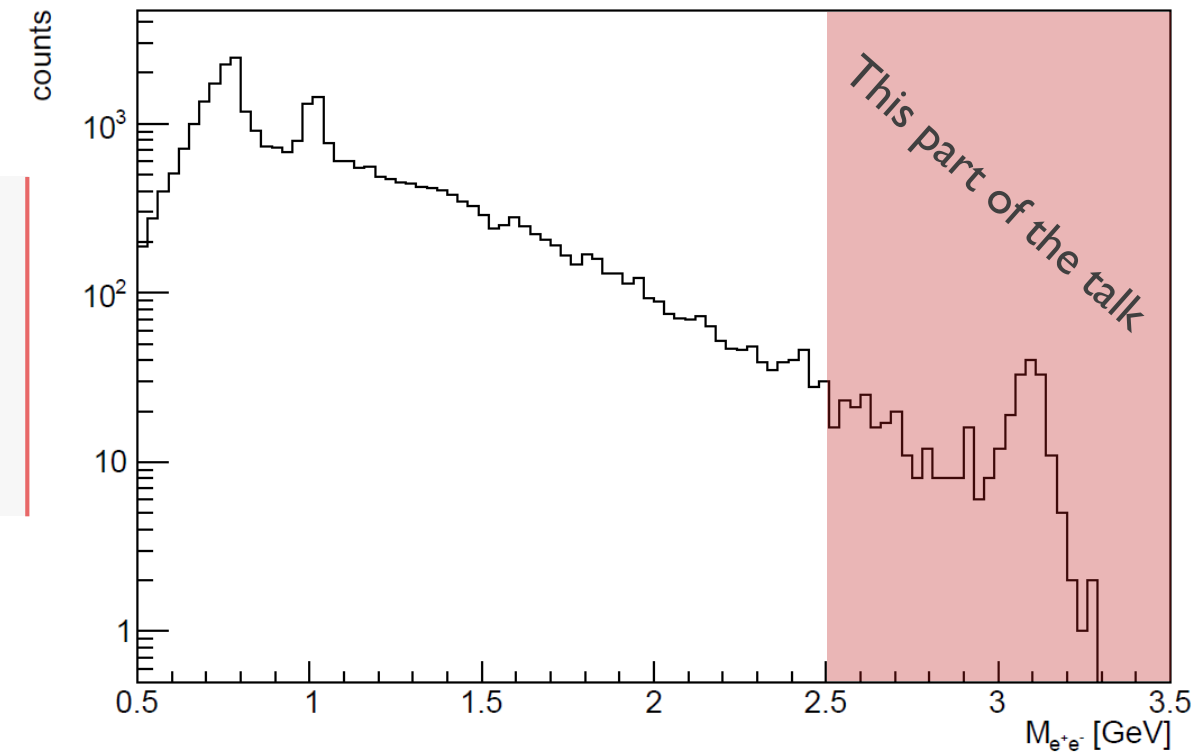
- Only a fraction of CLAS12 proton target dataset was used for in the PRL article (1/3).
- New significant improvement on the tracking software have been done since 2020 → 50% more efficiency for 3-particles final state



# Toward the measurement of the near threshold photo-production of J/ $\psi$ using CLAS12

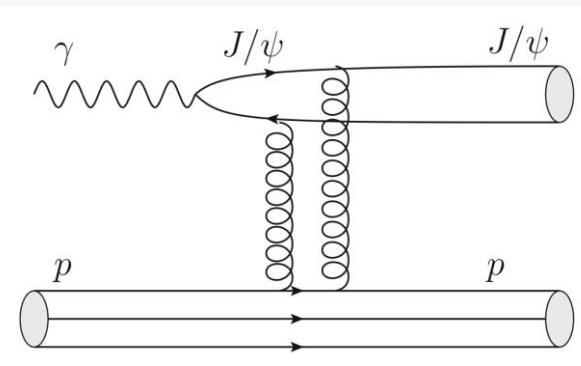
- Use the same dataset as for the TCS analysis for now.
- 10.6 GeV beam on Liquid H<sub>2</sub> target
- Accumulated charge: 37mC or 48 fb<sup>-1</sup>

CLAS12 Preliminary - ee ch.



# Motivations and results from other JLab experiments

- Probe the gluon content of the proton (under 2-gluon exchange assumption and no open-charm contributions discussed in the next slide)



- The  $t$ -dependence of the cross-section allow to access gluon Gravitational Form Factors (GFFs), mass radius of the nucleon and gluon GPDs.
- Model-dependent limit on the branching ration of the  $P_c$  pentaquark.

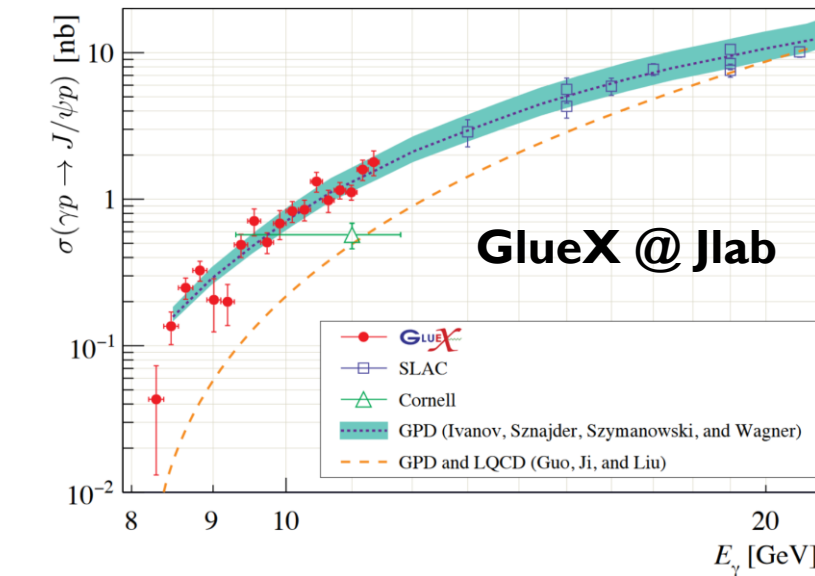
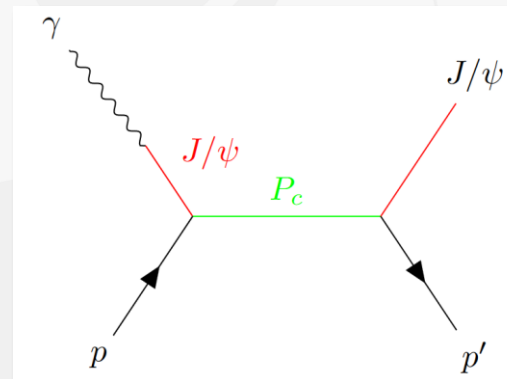


Figure in, Measurement of the  $J/\psi$  photoproduction cross section over the full near-threshold kinematic region, S. Adhikari et al. (GlueX Collaboration) arXiv:2304.03845

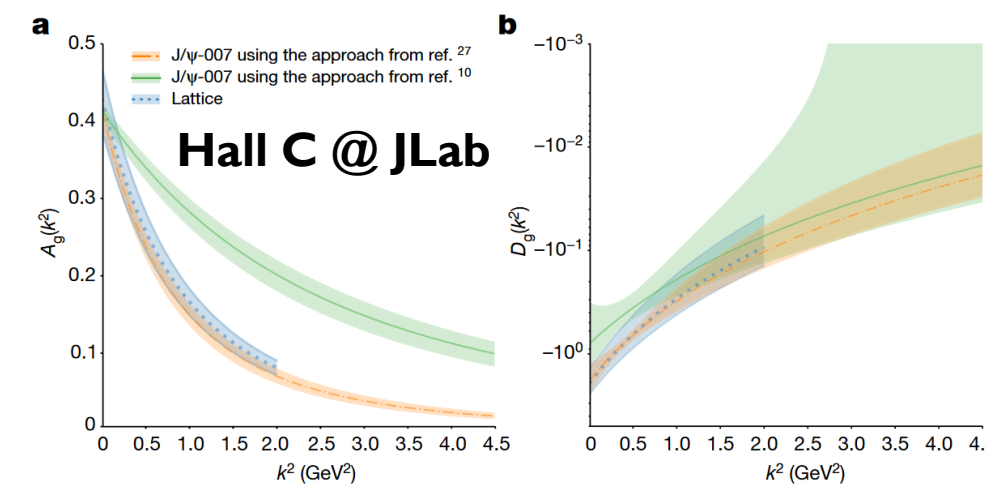


Figure in Duran, B., Meziani, ZE., Joosten, S. et al. Determining the gluonic gravitational form factors of the proton. *Nature* 615, 813–816 (2023)

# $J/\psi$ (quasi-)photoproduction events selection

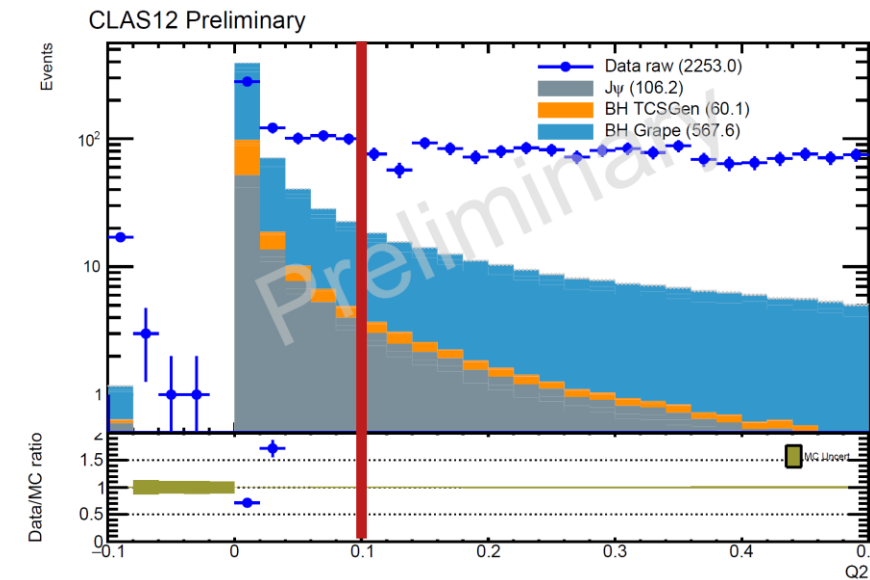
Can we do the same as for TCS ? In principle yes...

1) CLAS12 PID + Positron NN PID

$$ep \rightarrow (e')\gamma p \rightarrow (e')J/\psi p' \rightarrow (X)e^+e^-p'$$

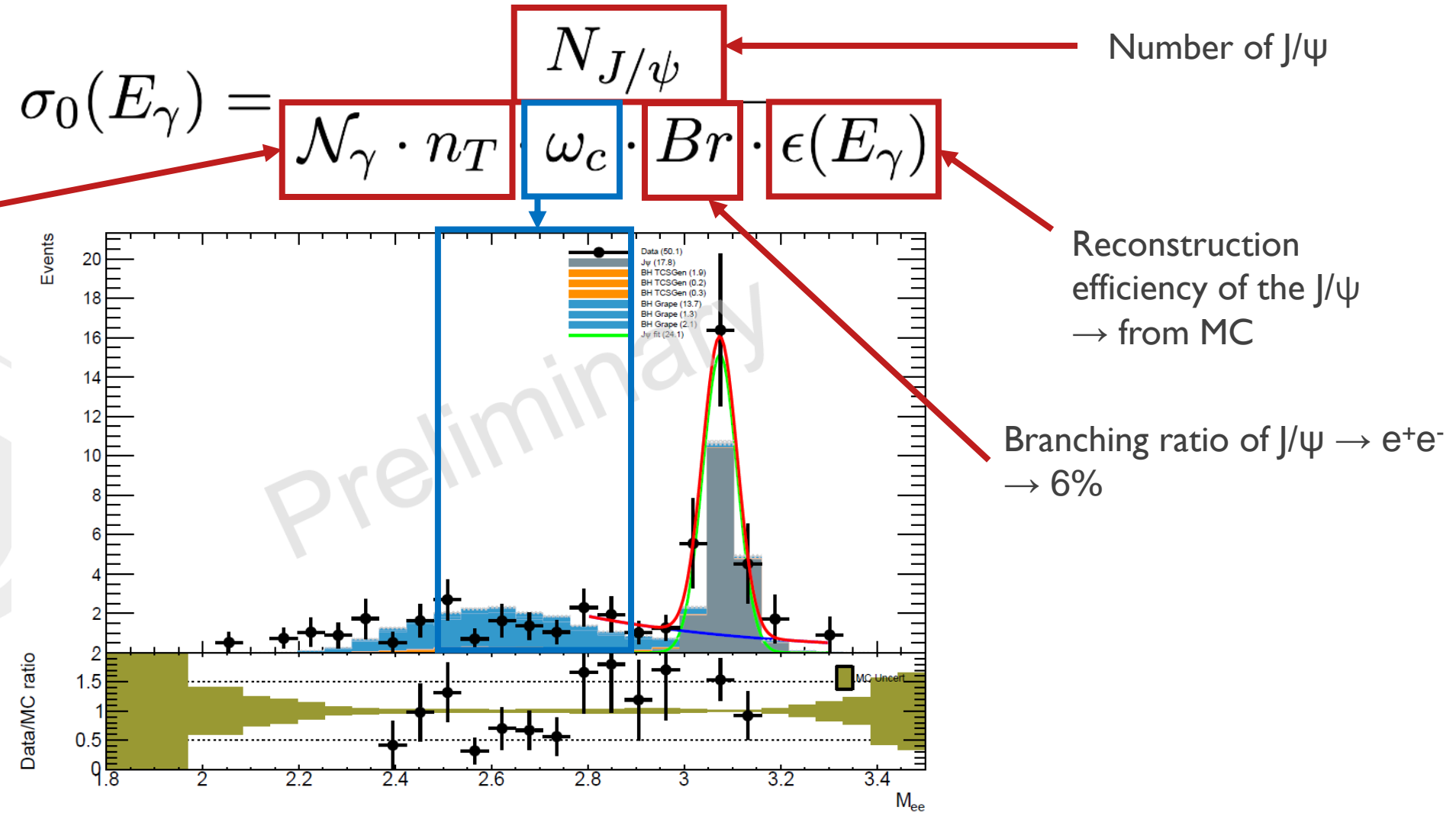
$p_X = p_{beam} + p_p - p_{e^+} - p_{e^+} - p_{p'} \rightarrow$  2)  $|M_X^2| < 0.4 GeV^2 \rightarrow$  3 )  $|Q^2| < 0.1$

- In practice, one wants to maximize the  $J/\psi$  yield.
- Reweighting procedure based on background estimation using same charge lepton events in both polarity of the CLAS12 torus magnet.



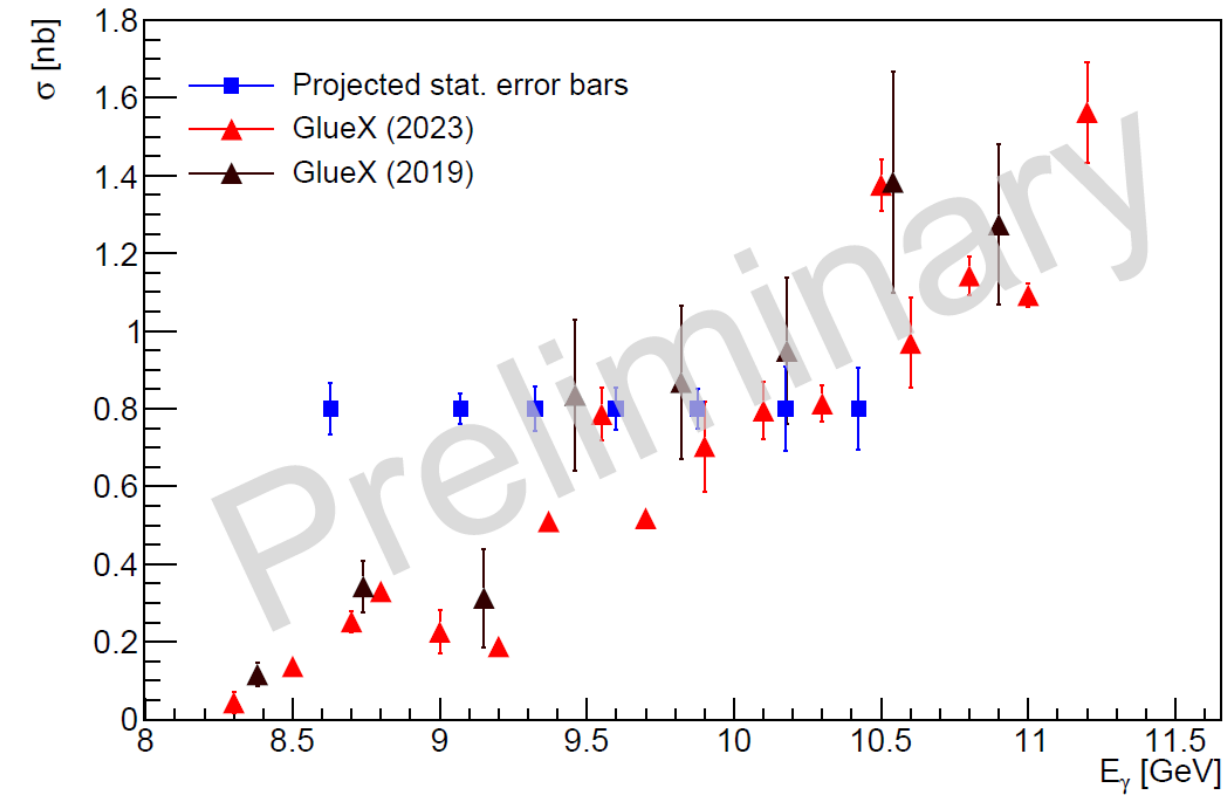
# Cross-section extraction

- Number of photons (from accumulated charge and photon flux from QED).
- Number of targets (from the density of dihydrogen and length of the target).



# Projections for the full CLAS12 proton target dataset

- Projected statistics error bars based on full dataset available on proton target and expected 50% improvement for tracking.
- Maximum photon energy slightly smaller than GlueX.
- Projected error bars are competitive with GlueX.
- $t$ -dependence will also be extracted.
- $J/\psi$  photoproduction on neutron is also measured, see Richard Tyson (Univ. of Glasgow) talk on Thursday.



Including all data taken on unpolarized proton and improved tracking efficiency

# Summary and take-aways

- The relation between GPDs and GFFs allows to probe the interaction.
- Dilepton final state reactions (TCS and J/ $\psi$ ) play a crucial role in experimentally extraction GFFs and GPDs.
- The CLAS12 detector is the ideal place to perform such measurement, with large angular coverage and great particle identification.
- First TCS measurement have been published in 2021, and the Forward/Backward asymmetry shows promising results. Full re-processed dataset will soon be analyzed.
- J/ $\psi$  photoproduction cross-section on proton target will soon be available. Stay tuned !

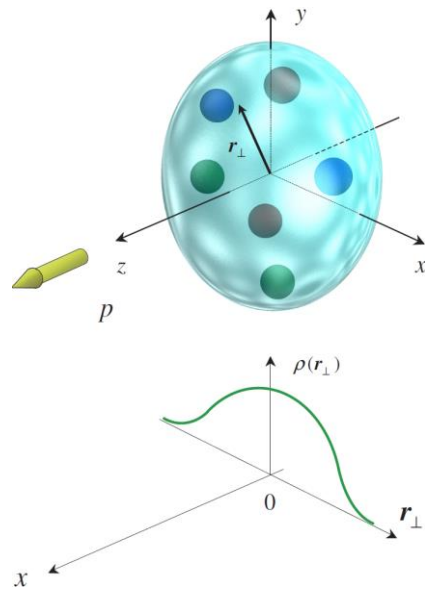
# BACK-UP



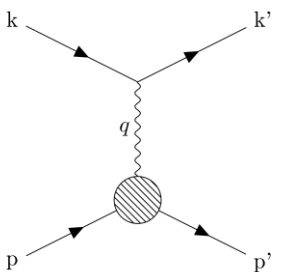
# GPDs and other theoretical considerations

# The Generalized Parton Distributions

## Form Factors



Accessed via elastic scattering

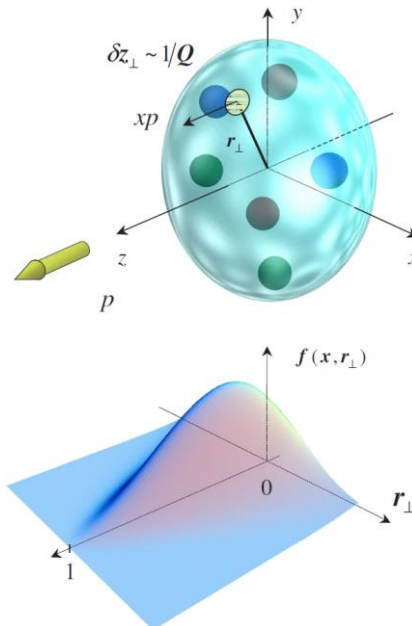


## Position in the transverse plane

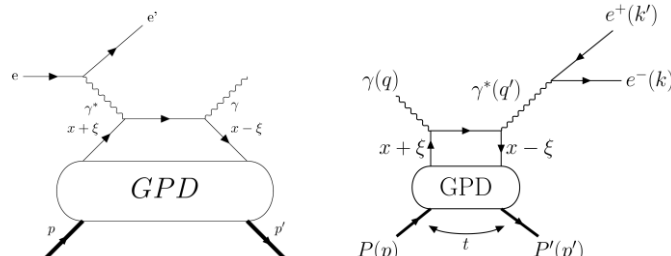
$$\int_{-1}^1 dx H^q(x, \xi, t) = F_1^q(t)$$

$$\int_{-1}^1 dx E^q(x, \xi, t) = F_2^q(t)$$

## GPDs



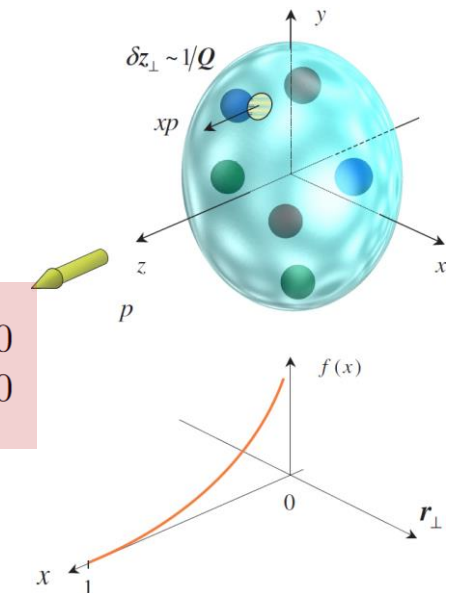
... and their correlations  
Accessed via exclusive reactions



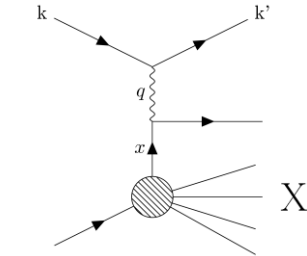
## Momentum in the longitudinal direction

$$H^q(x, 0, 0) = \begin{cases} q(x), & x > 0 \\ -\bar{q}(-x), & x < 0 \end{cases}$$

## PDFs



Accessed via Deep Inelastic Scattering



Figures in A.V. Belitsky, A.V. Radyushkin, Unraveling hadron structure with generalized parton distributions, Physics Reports, Volume 418, Issues 1–6 2005

# What can we learn from GPDs ?

- Tomography of the nucleon: the Fourier transform of the GPDs can be interpreted as a probability density:

$$H^q(x, b_\perp) = \int \frac{d^2 \Delta_\perp}{(2\pi)^2} e^{-ib_\perp \Delta_\perp} H^q(x, 0, -\Delta_\perp^2)$$

- Understanding the spin composition of the nucleon (aka the “spin puzzle”) using the Ji’s sum rule:

$$\frac{1}{2} = J_Q + J_G \longrightarrow J_Q = \sum_q \frac{1}{2} \int_{-1}^1 dx x(H^q(x, \xi, 0) + E^q(x, \xi, 0)) = \sum_q \frac{1}{2} (A^q(t) + B^q(t))$$

- Accessing Gravitational Form Factors by mimicking a spin-2 interaction:

$$\int_{-1}^1 dx xH^q(x, \xi, t) = A^q(t) + \xi^2 D^q(t) \quad \int_{-1}^1 dx xE^q(x, \xi, t) = B^q(t) - \xi^2 D^q(t)$$

# Motivations to measure $J/\psi$ photoproduction near threshold: the open-charm “issue”

## Open-charm “issue”

- The previous considerations rely on the application of Vector Meson Dominance.
- Thus the contribution from open-charm meson channels must be ruled-out/understood.
- Measuring photoproduction on both proton and neutron probes different channel and will bring new constraints on open-charm contributions.

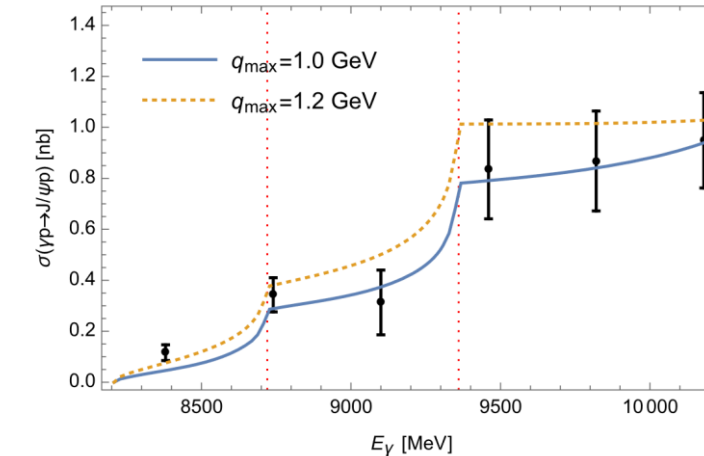
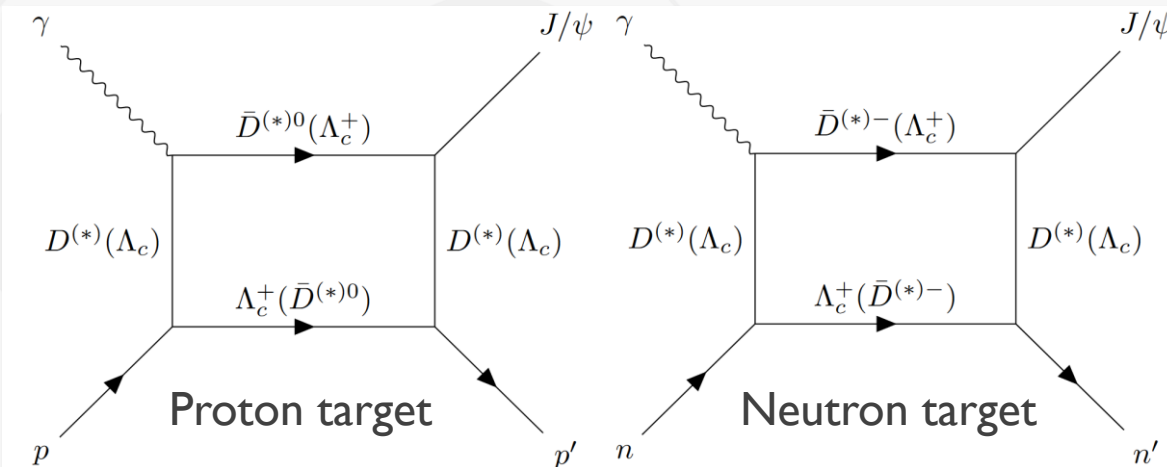


Figure in Du, ML., Baru, V., Guo, FK. et al. Deciphering the mechanism of near-threshold  $J/\psi$  photoproduction. *Eur. Phys. J. C* 80, 1053 (2020)

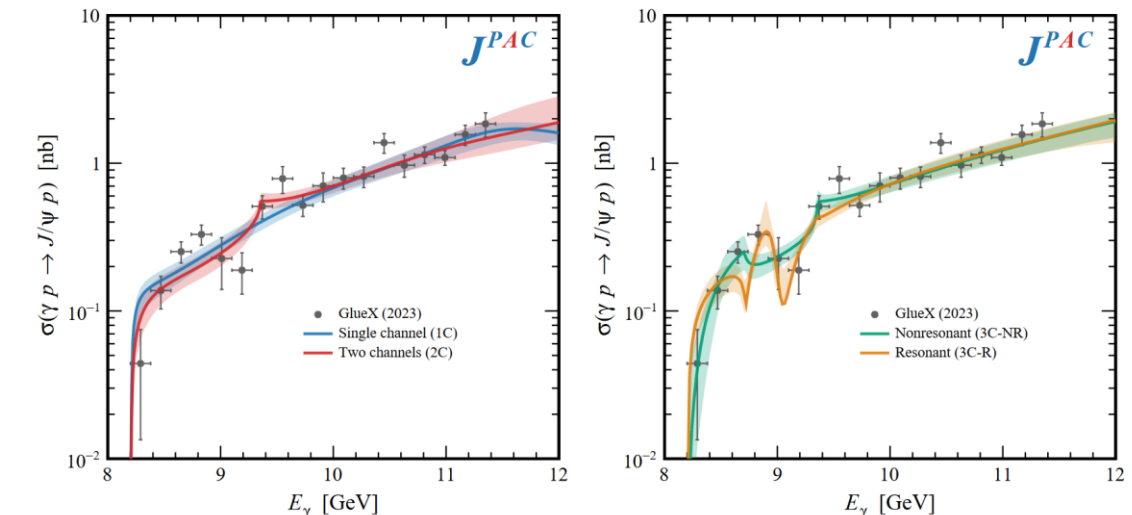


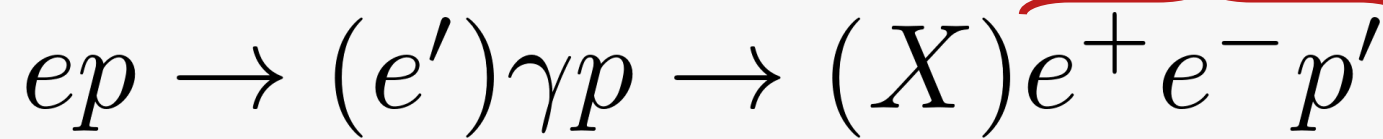
Figure in D. Winney, C. Fernandez-Ramirez, A. Pilloni, A. N. Hiller Blin et al. (JPAC), Dynamics in near-threshold  $J/\psi$  photoproduction [arXiv:2305.01449](https://arxiv.org/abs/2305.01449)

# Event selection

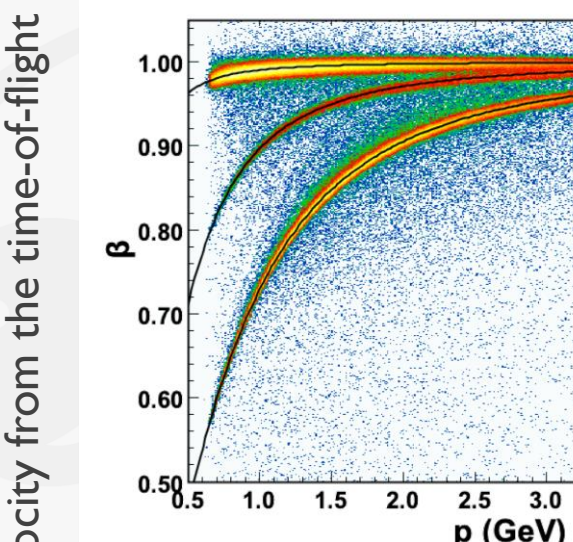


# Particle identification

1) CLAS12 PID + Positron NN PID



## Proton identification

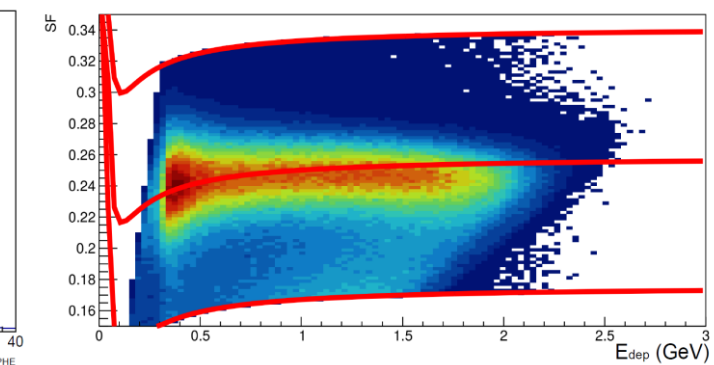
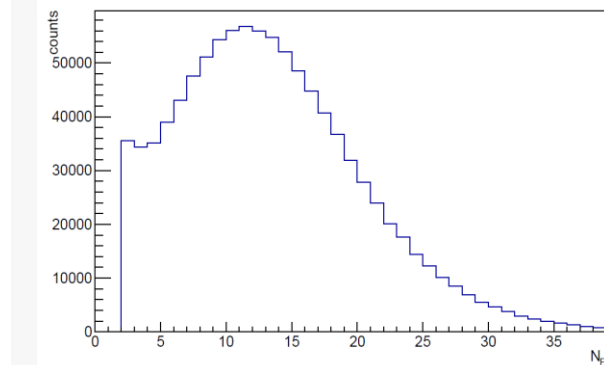


Momentum from the track curvature

## Lepton identification

Cherenkov counters

+ Calorimeter energy deposition

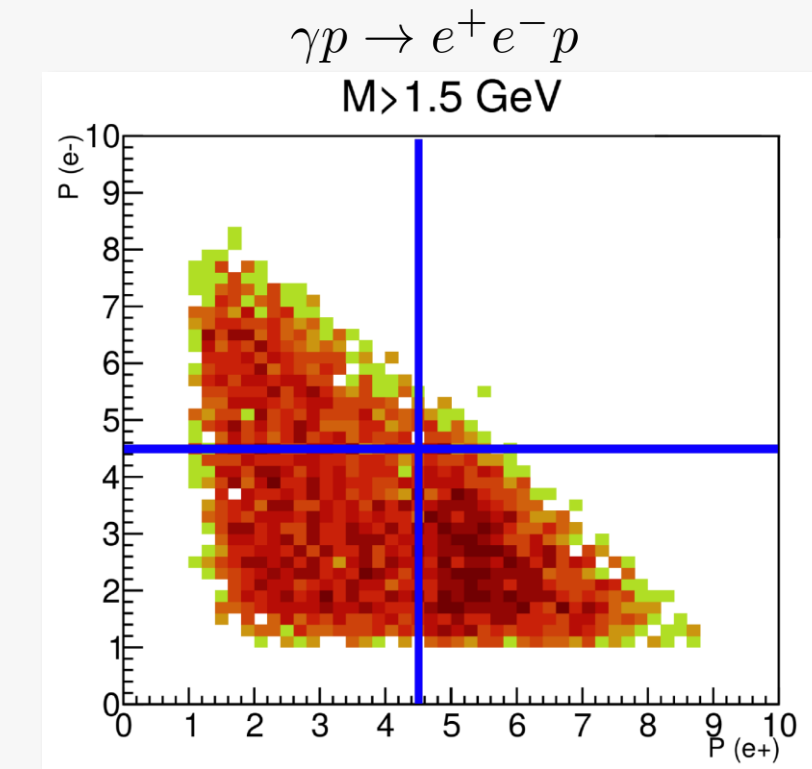
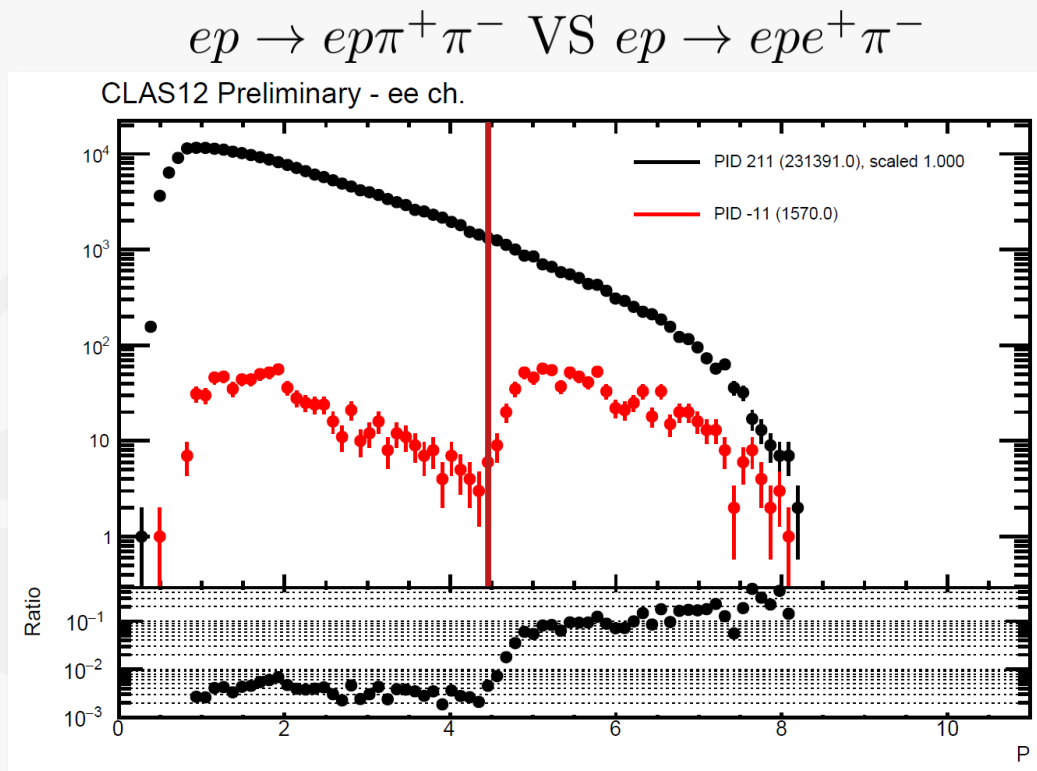


$$\text{Sampling Fraction} = \frac{E_{dep}}{P}$$

# One important challenge: a clean positron identification

## Pion background at large momenta

At high momenta (typically above the HTCC threshold at 4.5 GeV), both pions and leptons will emit Cherenkov light.



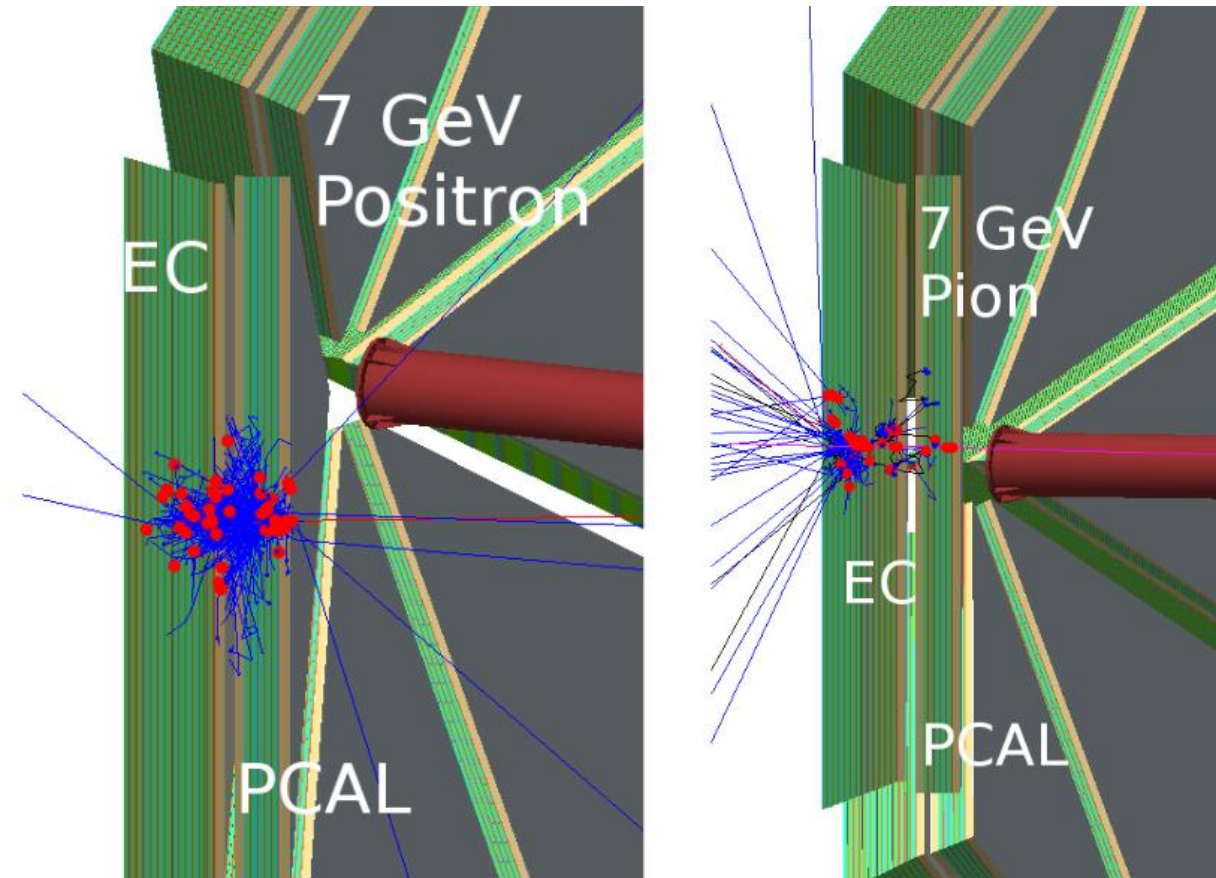
# AI identification of the positrons

## Strategy and discriminating variables

- Leptons produce electromagnetic showers and tend to deposit energy in the first layers of the calorimeters.
- Pions are **Minimum Ionizing Particles** in the GeV region, they deposit small amounts of energy all along their path.
- Two main characteristics to use:

1.  $SF_{EC \text{ Layer}} = \frac{E_{dep}(\text{EC Layer})}{P}$

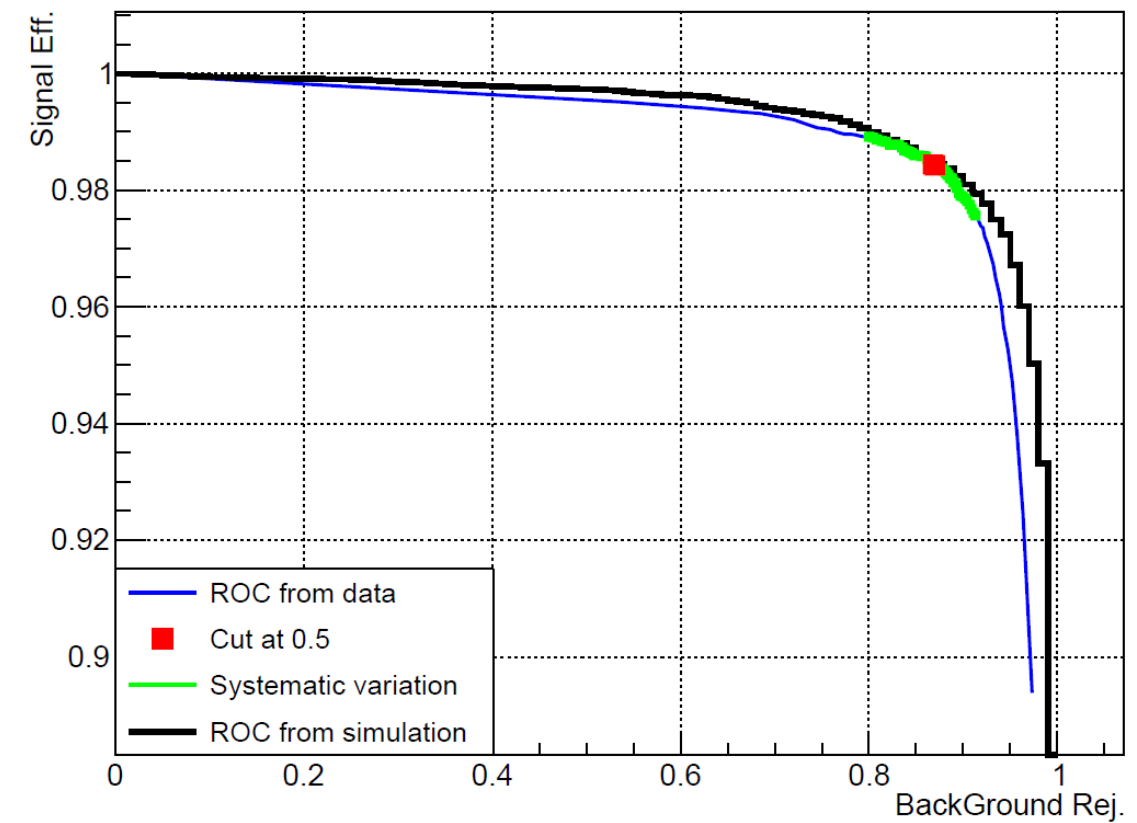
2.  $M_2 = \frac{1}{3} \sum_{U,V,W} \frac{\sum_{\text{strip}} (x - D)^2 \cdot \ln(E)}{\sum_{\text{strip}} \ln(E)}$



# Performances of AI identification of the positrons

## Strategy and discriminating variables

- Leptons produce electromagnetic showers and tend to deposit energy in the first layers of the calorimeters.
- Pions are **Minimum Ionizing Particles** in the GeV region, they deposit small amounts of energy all along their path.
- Two main characteristics to use:
  1.  $SF_{EC\ Layer} = \frac{E_{dep}(EC\ Layer)}{P}$
  2.  $M_2 = \frac{1}{3} \sum_{U,V,W} \frac{\sum_{strip} (x-D)^2 \cdot \ln(E)}{\sum_{strip} \ln(E)}$



# More on TCS



# TCS interference cross-section formulae and CFFs

## Unpolarized cross-section

Formulae and notations of Berger, Diehl, Pire, Eur.Phys.J.C23:675-689,2002

$$\frac{d^4\sigma_{INT}}{dQ'^2 dt d\Omega} \propto \frac{L_0}{L} \left[ \cos(\phi) \frac{1 + \cos^2(\theta)}{\sin(\theta)} \text{Re} \tilde{M}^{--} + \dots \right]$$

$$\rightarrow \tilde{M}^{--} = \frac{2\sqrt{t_0 - t}}{M} \frac{1 - \xi}{1 + \xi} \left[ F_1 \mathcal{H} - \xi(F_1 + F_2) \tilde{\mathcal{H}} - \frac{t}{4M^2} F_2 \mathcal{E} \right]$$

## Compton Form Factors (CFFs)

$$\mathcal{H} = \int_{-1}^1 H(x, \xi, t) \left( \frac{1}{\xi - x - i\epsilon} - \frac{1}{\xi + x - i\epsilon} \right)$$

## Polarized cross-section

$$\frac{d^4\sigma_{INT}}{dQ'^2 dt d\Omega} = \frac{d^4\sigma_{INT}|_{\text{unpol.}}}{dQ'^2 dt d\Omega} - \nu \cdot A \frac{L_0}{L} \left[ \sin(\phi) \frac{1 + \cos^2(\theta)}{\sin(\theta)} \text{Im} \tilde{M}^{--} + \dots \right]$$

# First observable: the photon polarization asymmetry

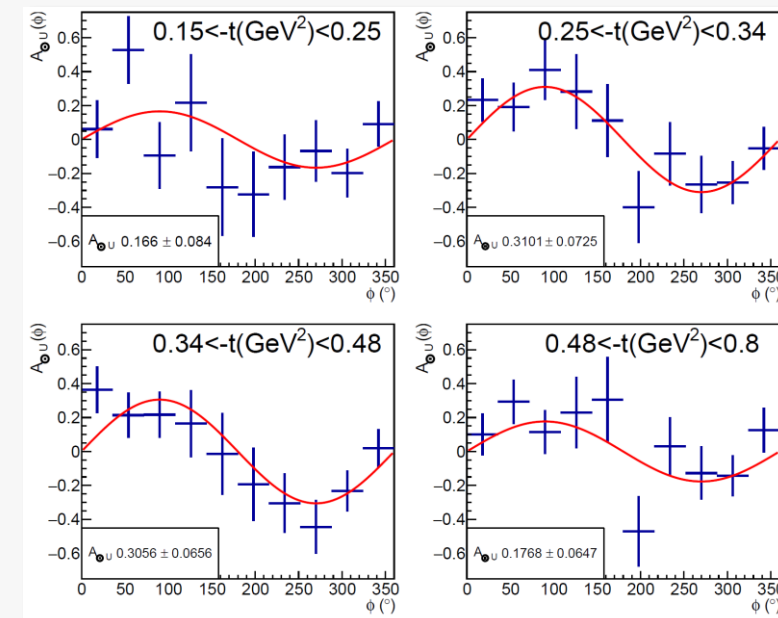
## Definition

$$A_{\odot U} = \frac{d\sigma^+ - d\sigma^-}{d\sigma^+ + d\sigma^-} = \frac{-\frac{\alpha_e^3 m_p}{4\pi s^2} \frac{1}{-t} \frac{1}{Q'} \frac{1}{\tau\sqrt{1-\tau}} \frac{L_0}{L} \sin \phi \frac{(1+\cos^2 \theta)}{\sin(\theta)} \text{Im } \tilde{M}^{--}}{d\sigma_{BH}}$$

## Measurement

$$A_{\odot U}(-t, E\gamma, M; \phi) = \frac{1}{P_b} \frac{N^+ - N^-}{N^+ + N^-} \text{ where } N^\pm = \sum \frac{1}{Acc} P_{trans.}$$

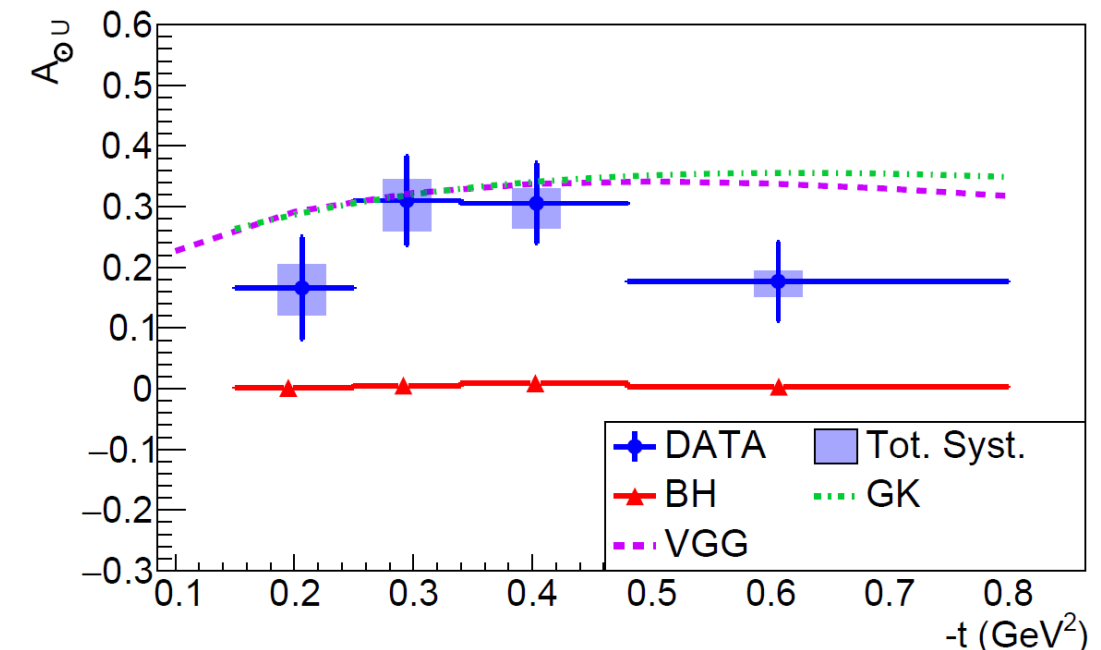
- $P_{trans.}$  is the transferred polarization from the electron to the photon, fully calculable in QED.  
Olsen, Maximon, Phys. Rev. 114 (1959)
- $P_b$  is the polarization of the electron beam at 85%.
- The obtained distributions of  $A_{\odot U}(-t; \phi)$  are then fitted with a sine function.



# Photon polarization asymmetry results

- A sizeable asymmetry is measured, above the expected vanishing asymmetry predicted for BH.
- Results have been compared to 2 model predictions:
  1. VGG model
  2. GK model
- The size of the asymmetry is well reproduced by both models, giving a hint for the universality of GPDs.

$\langle M \rangle = 1.8 \text{ GeV}; \langle E_\gamma \rangle = 7.29 \text{ GeV};$   
 $\langle \theta \rangle = 92^\circ$



# J/ $\psi$ analysis



# Background subtracted data using same-charge lepton events

- Opposite charge leptons

Background final states ( $\pi^+ \rightarrow e^+$ )

$$e' p' e^+ (e^- + X) + e' p' \pi^+ (\pi^- + X)$$

$$N(e^+ e^- p') = n_S(e^+ e^-) + n_{BG}(e' e^+ / \pi^+)$$

Physics final state

$$e^- e^+ p'(e')$$

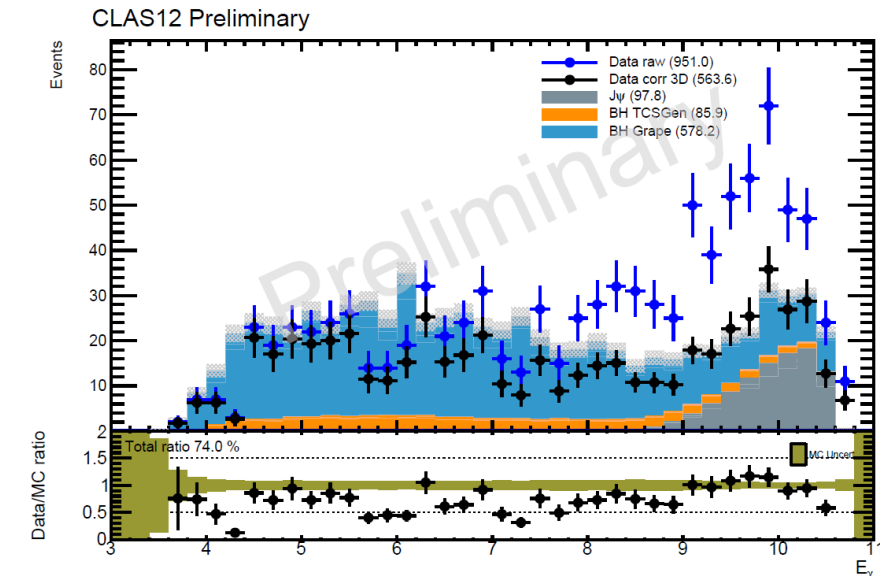
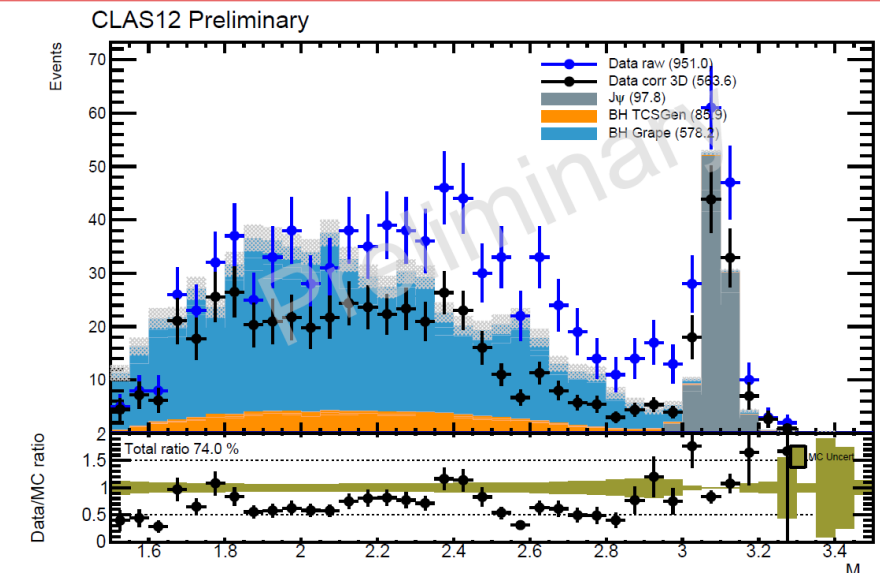
- Same charge leptons

$$ep \rightarrow p' e^- e^- (X \simeq e)$$

$$e' p' \pi^- (\pi^+ + X) + e' p' e^- (e^+ + X)$$

- Background correction weight, combining inbending and outbending data:

$$w = \frac{n_S}{(n_S + n_{BG})} = 1 - \sqrt{\left| \frac{N_{e^- e^- p}}{N_{e^+ e^- p}} \right|_{In} \left| \frac{N_{e^- e^- p}}{N_{e^+ e^- p}} \right|_{Out}}$$



# Background removal procedure

## Sample contents

### Opposite charge leptons

Background final states ( $\pi^+ \rightarrow e^+$ )

$$e' p' e^+ (e^- + X) + e' p' \pi^+ (\pi^- + X)$$

$$N(e^+ e^- p') = n_S(e^+ e^-) + n_{BG}(e' e^+ / \pi^+)$$

Physics final state

$$e^- e^+ p'(e')$$

### Same charge leptons

$$ep \rightarrow p' e^- e^- (X \simeq e)$$

$$e' p' \pi^- (\pi^+ + X) + e' p' e^- (e^+ + X)$$

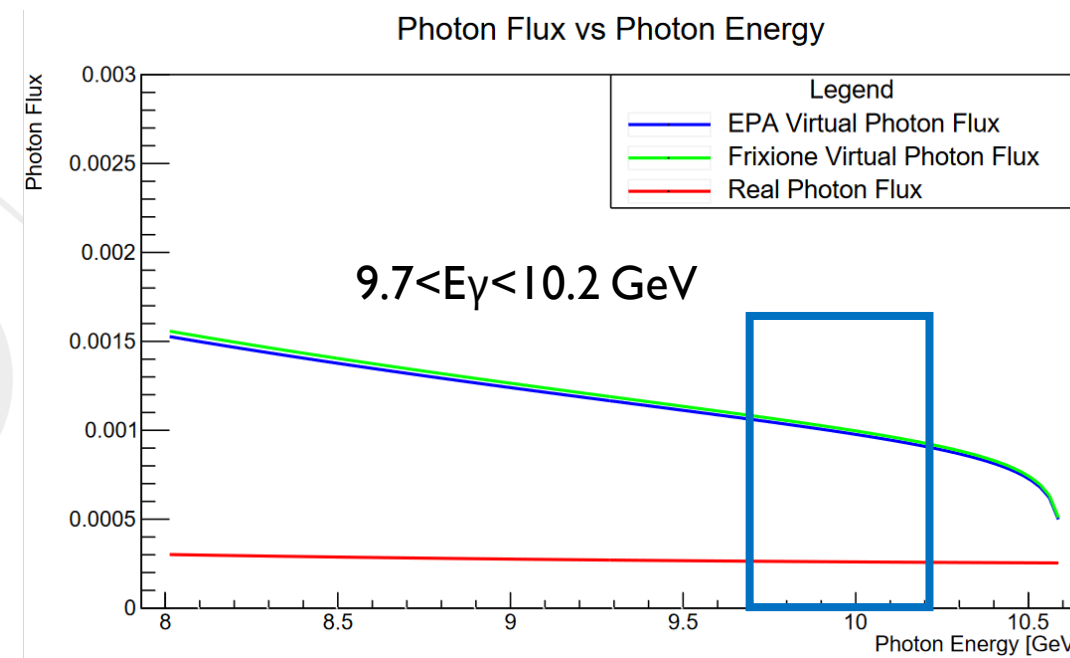
$$\begin{aligned} R^{in} &= \frac{N^{in}(e' e^- p')}{N^{in}(e^+ e^- p')} = \frac{a^2 \cdot \sigma_{BG}}{a \cdot b \cdot \sigma_{BG+S}} = \frac{a \cdot \sigma_{BG}}{b \cdot \sigma_{BG+S}} \\ R^{out} &= \frac{N^{out}(e' e^- p')}{N^{out}(e^+ e^- p')} = \frac{b^2 \cdot \sigma_{BG}}{a \cdot b \cdot \sigma_{BG+S}} = \frac{b \cdot \sigma_{BG}}{a \cdot \sigma_{BG+S}} \end{aligned}$$

$$w = \frac{S}{(S + B)_{In}} = 1 - \frac{N_{e^- e^- p}}{N_{e^- e^+ p}{}_{In}} \frac{b}{a} = 1 - \sqrt{\frac{N_{e^- e^- p}}{N_{e^- e^+ p}{}_{In}} \frac{N_{e^- e^- p}}{N_{e^- e^+ p}{}_{Out}}}$$

# Photon flux and accumulated charge

$$\sigma_0(E_\gamma) = \frac{N_{J/\psi}}{\mathcal{N}_\gamma \cdot n_T \cdot \omega_c \cdot Br \cdot \epsilon(E_\gamma)}$$

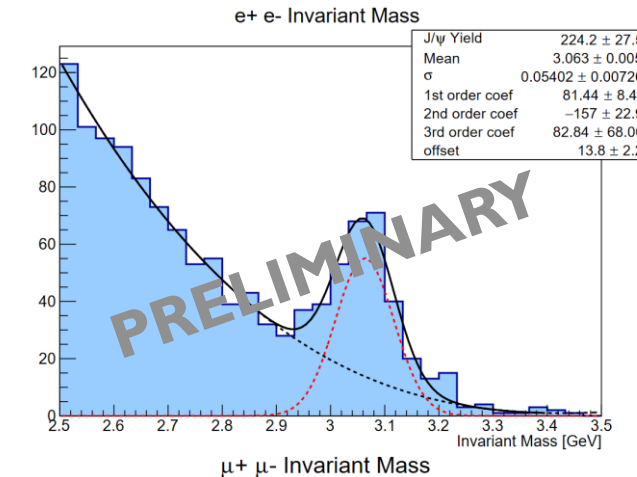
- Number of photons (from accumulated charge and photon flux from QED)
- Number of targets (from the density of dihydrogen and length of the target)



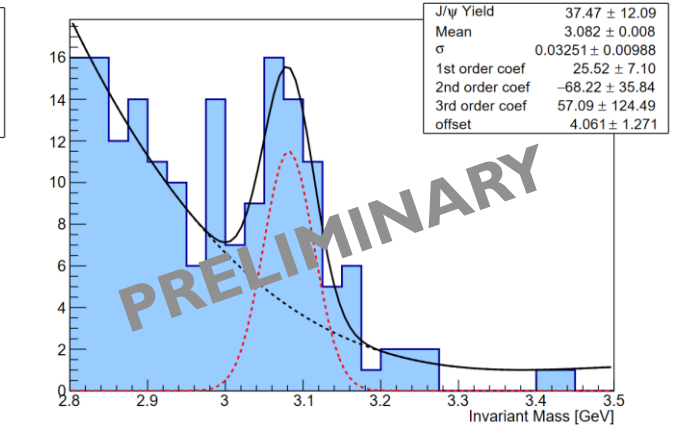
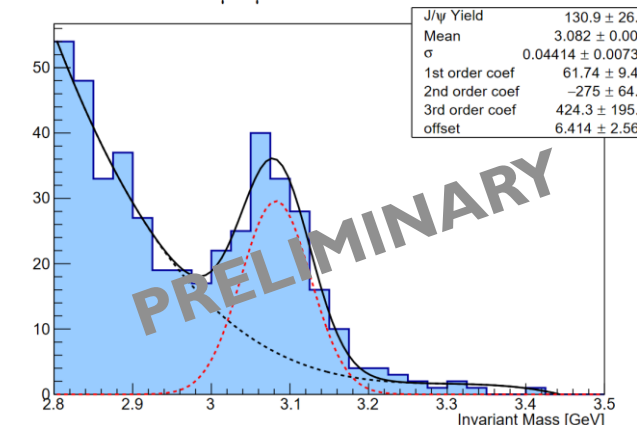
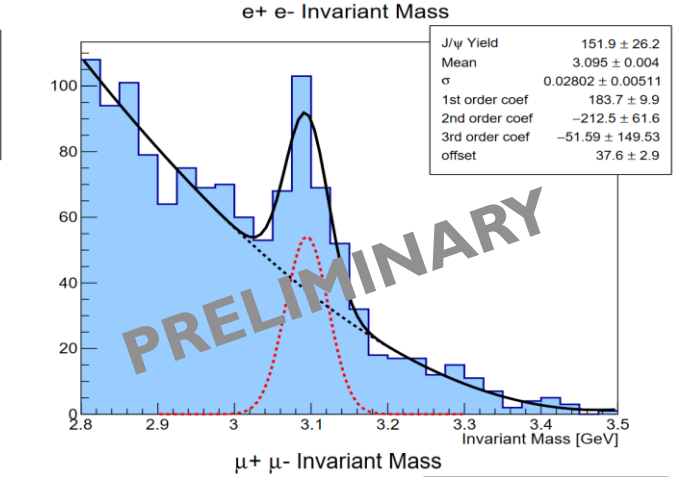
# Deuterium target and muon final state

- Deuterium data were taken by CLAS12 in 2019/2020.
- Opportunity to measure  $J/\psi$  production on (bound) neutron and (bound) proton.
- Alongside this analysis, a framework to explore the muon decay channel was developed.
- This effort is lead by R.Tyson from University of Glasgow.

Bound proton



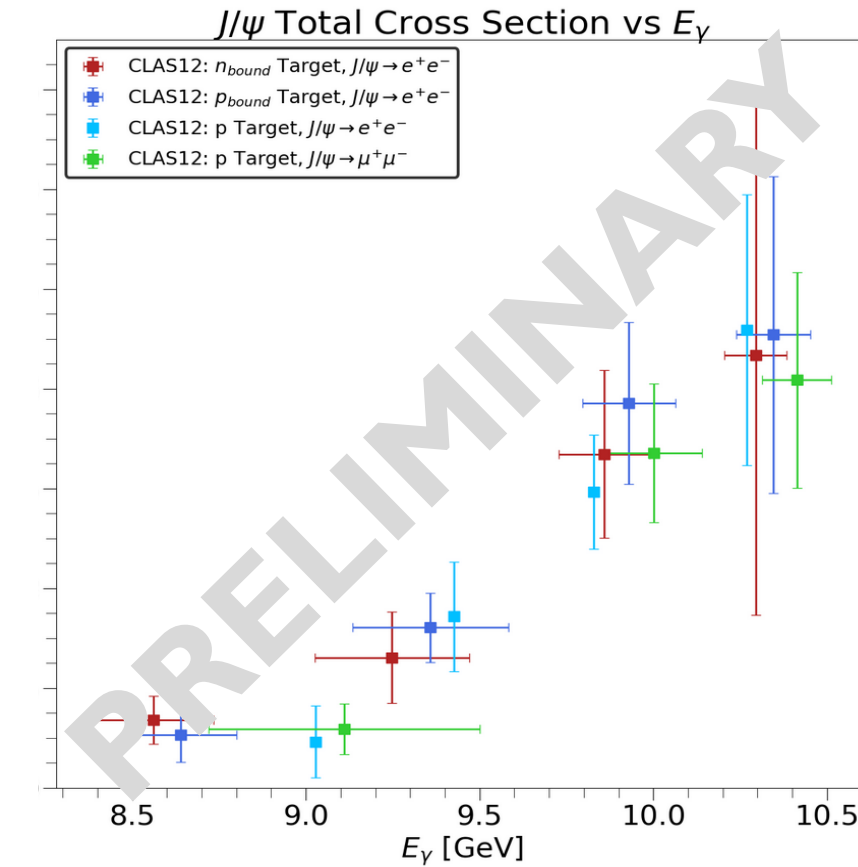
Bound neutron



Taken from R.Tyson PhD analysis, Univ. of Glasgow

# Preliminary results for proton/neutron data

- Preliminary results for the comparison of decay channels and target nucleon.
- This measurement could have implication on understanding open-charm channels contribution.

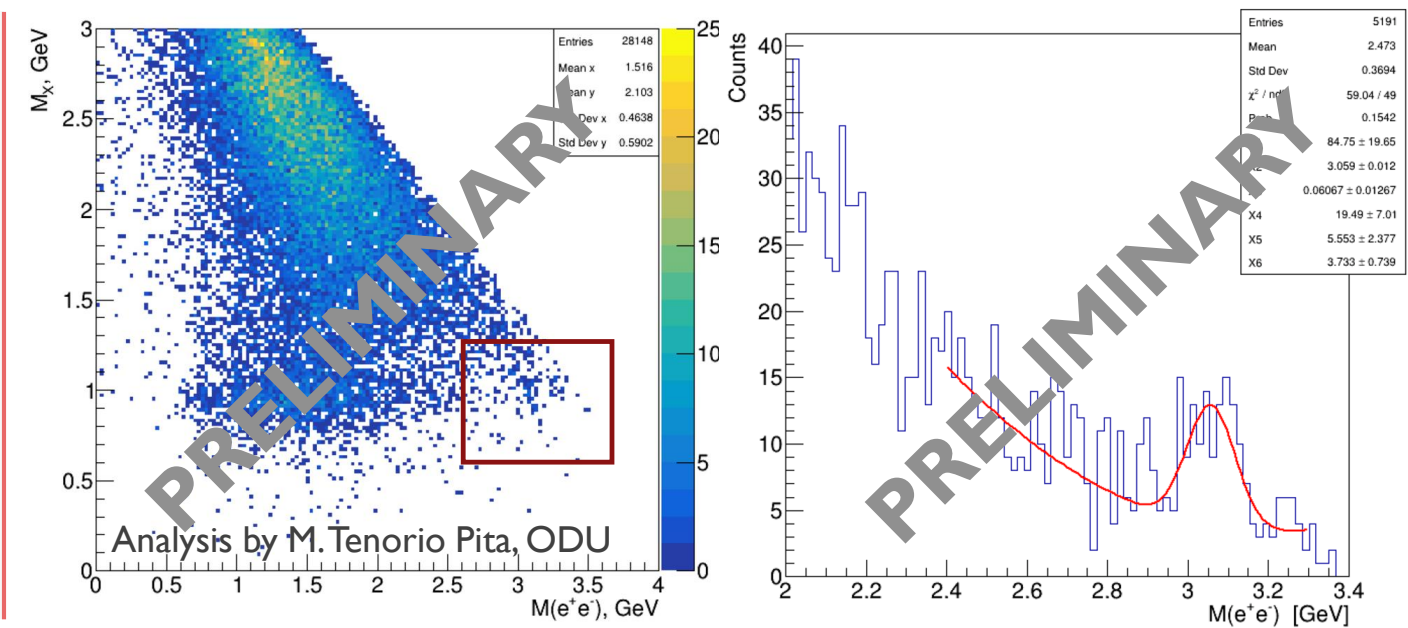


Taken from R.Tyson PhD analysis, Univ. of Glasgow

# Tagged J/ $\psi$ quasi-photoproduction analysis

$$ep \rightarrow e' J/\psi \ p' \rightarrow e' l^+ l^- (X)$$

- Analysis conducted by M.Tenorio Pita, ODU.
- In this case, one electron in the Forward Tagger (Low lab angle  $<5^\circ$ ) and a lepton pair in CLAS12.
- Excellent cross-check of the quasi-photoproduction approach.
- Early results show low statistics, the new data “cooking” including better tracking efficiency will be beneficial for this analysis.
- Other event topologies will be explored.



## Other potential J/ $\psi$ analysis using CLAS12 data

- Available data for longitudinally polarized proton target